PHYSICAL REVIEW B **81**, 104427 (2010)

Effects of substrate-induced strain on transport properties of $LaMnO_{3+\delta}$ and $CaMnO_3$ thin films using ferroelectric poling and converse piezoelectric effect

R. K. Zheng,[1,2] H.-U. Habermeier,[1] H. L. W. Chan,[2] C. L. Choy,[2] and H. S. Luo[3]

[1]*Max Planck Institute for Solid State Research, Heisenbergstrasse 1, D-70569 Stuttgart, Germany*

[2]*Department of Applied Physics and Materials Research Center, The Hong Kong Polytechnic University, Hong Kong, China*

[3]*State Key Laboratory of High Performance Ceramics and Superfine Microstructure, Shanghai Institute of Ceramics, Chinese Academy of Sciences, Shanghai 201800, China*

(Received 19 September 2009; revised manuscript received 8 February 2010; published 30 March 2010)

We have investigated the effects of the strain induced by ferroelectric poling (or the converse piezoelectric effect) on the transport properties of $LaMnO_{3+\delta}$ and $CaMnO_3$ thin films grown on ferroelectric $0.67Pb(Mg_{1/3}Nb_{2/3})O_3$-$0.33PbTiO_3$ single-crystal substrates. The ferroelectric poling of the substrate gives rise to a reduction in the in-plane tensile strain of the $LaMnO_{3+\delta}$ film, which results in a significant decrease in the resistance and increase in the insulator-to-metal transition temperature T_P of the film. The ferroelectric poling also leads to opposite effects on the magnetoresistance (MR) below and above T_P, namely, MR is reduced for $T<T_P$ while MR is enhanced for $T>T_P$. These strain effects are explained in terms of coexisting phases whose volume fractions are modified as a result of the reduction in the Jahn-Teller (JT) distortion due to ferroelectric poling. An investigation of the effects of the strain induced by the converse piezoelectric effect on the resistance of the $LaMnO_{3+\delta}$ and $CaMnO_3$ films shows that the resistance-strain coefficients $(\Delta R/R)/(\Delta c_{film}/c_{film})$ of the $LaMnO_{3+\delta}$ film is much larger than those of the $CaMnO_3$ film. This result may imply that the strain-induced modification of the electronic bandwidth alone cannot account for the large $(\Delta R/R)/(\Delta c_{film}/c_{film})$ observed in the $LaMnO_{3+\delta}$ film, and highlights that the strong coupling of charge carriers to JT distortion is crucial for understanding the effects of the substrate-induced strain in manganite thin films.

DOI: 10.1103/PhysRevB.81.104427 PACS number(s): 75.47.Lx, 75.47.Gk, 77.65.−j, 77.80.−e

I. INTRODUCTION

Lanthanum-based mixed-valent manganites $La_{1-x}A_xMnO_3$ (A=Ca, Sr, and Ba) have attracted considerable attention in the last decade due to their interesting physical properties and potential device applications.[1] The parent compound, $LaMnO_3$, is an insulating material which shows simultaneous cooperative Jahn-Teller (JT) distortion of MnO_6 octahedra and $d_{3x^2-r^2}/d_{3y^2-r^2}$ orbital order below T_{JT}=750 K.[2] Quite a number of experimental studies have shown that $LaMnO_3$ compounds exhibit a wide range of oxygen nonstoichiometry,[3–8] as reflected in the general formula $LaMnO_{3+\delta}$. The excess of oxygen causes the valence state of a portion of the manganese ions to change from Mn^{3+} to Mn^{4+} and thus suppresses the cooperative JT distortion and $d_{3x^2-r^2}/d_{3y^2-r^2}$ orbital ordering, which consequently results in substantial changes in the structural, magnetic, and transport properties of $LaMnO_{3+\delta}$ compounds.[3–7]

As δ increases, the crystallographic structure evolves from the highly JT distorted orthorhombic structure (*Pbmn*, $c/\sqrt{2}<a<b$) for $0\leq\delta\leq0.04$ to the slightly JT-distorted orthorhombic structure (*Pbmn*, $a\leq c/\sqrt{2}<b$), and subsequently, to the rhombohedral structure for $\delta>0.1$.[3,4] At the same time, the magnetic ground state evolves from the canted antiferromagnetic (AFM) for $\delta<0.05$ to mixed AFM ferromagnetic (FM) for $0.05\leq\delta\leq0.11$, and then to FM for $0.11<\delta\leq0.14$, and finally to metamagnetic canted-spin configuration for $0.14<\delta\leq0.18$.[5] For the transport properties, controversial results have been reported for close δ, Ritter *et al.*[3] and Louca *et al.*[6] reported that the δ=0.1 compound has a rhombohedral crystallographic symmetry and $T_C\sim150-155$ K while Choi *et al.*[7] reported that the δ=0.096 compound has a orthorhombic crystallographic symmetry and $T_C\sim186$ K. All these results demonstrate that the properties of nonstoichiometric $LaMnO_{3+\delta}$ compounds are very sensitive to the excess of oxygen. Therefore, when one studies the strain effects of $LaMnO_{3+\delta}$ thin films, it is very important that the investigated $LaMnO_{3+\delta}$ films have the same δ since the properties of $LaMnO_{3+\delta}$ is so sensitive to δ.

Ritter *et al.*[3] performed measurements of ac initial magnetic susceptibility, magnetization, magnetoresistance (MR), and neutron-diffraction measurements on a series of $LaMnO_{3+\delta}$ samples and found that, as δ increases from 0 to 0.07, a small fraction of FM metallic phase appears due to the local Mn^{3+}-O-Mn^{4+} double exchange interaction. The local FM metallic phase coexists with the AFM insulating phase. They further found that for δ=0.07 and 0.1 samples, charge-ordered (CO) phase emerges at low temperatures below ~110 K, well below the ferromagnetic ordering temperature (~150 K), pointing to the coexistence of CO phase and FM metallic phase at low temperatures. Since the JT distortion plays a very important role in localizing the e_g electrons, it is expected that a change in the magnitude of the JT distortion would lead to significant changes in the volume fraction of the coexistence phases and hence the transport and magnetic properties of the $LaMnO_{3+\delta}$ compounds.

Although the properties of $LaMnO_{3+\delta}$ compounds in bulk form have been studied extensively, investigations on the properties of nonstoichiometric $LaMnO_{3+\delta}$ thin films are very limited. Particularly, the effects of substrate-induced strain on the JT distortion and phase separation in $LaMnO_{3+\delta}$ thin films are still unknown. In this work, we deposited

$LaMnO_{3+\delta}$ films (for which the JT distortion is significant) and $CaMnO_3$ films (for which there is no JT distortion) on ferroelectric $0.67Pb(Mg_{1/3}Nb_{2/3})O_3$-$0.33PbTiO_3$ (PMN-PT) single-crystal substrates whose in-plane strain can be dynamically changed via ferroelectric poling or the converse piezoelectric effect[9–15] and studied the effects of the strain induced by ferroelectric poling or the converse piezoelectric effect on the JT distortion, phase separation, and transport properties of the films. Since we dynamically change the strain state of the films using the same $LaMnO_{3+\delta}$/PMN-PT or $CaMnO_3$/PMN-PT sample, therefore the effects of oxygen nonstoichiometry δ on the properties of the films are kept constant.

We have observed that the induced strain in the PMN-PT substrate was effectively transferred to the film, causing a reduction in the in-plane tensile strain of the $LaMnO_{3+\delta}$ film. Consequently, the JT distortion, phase separation, and transport properties of the $LaMnO_{3+\delta}$ film are modified. Moreover, we give experimental evidence that the electron-lattice coupling due to the JT distortion plays a crucial role in determining the substrate-induced strain effects in $LaMnO_{3+\delta}$ films by comparing the resistance-strain coefficients $(\Delta R/R)/(\Delta c_{film}/c_{film})$ of $LaMnO_{3+\delta}$ films with those of $CaMnO_3$ films.

II. EXPERIMENTAL DETAILS

PMN-PT single crystals with dimensions of $\Phi 48 \times 80$ mm^2 were grown by a modified Bridgman technique[16] at the Shanghai Institute of Ceramics. The crystals were cut into rectangular plates ($10 \times 2.5 \times 0.5$ mm^3) with the plate normal in the $\langle 001 \rangle$ crystal direction and polished to a surface roughness of less than 1 nm. $LaMnO_{3+\delta}$ and $CaMnO_3$ films were deposited on the (001)-oriented and polished PMN-PT substrates using dc magnetron sputtering. The deposition was carried out in an argon-oxygen flow with 60% Ar and 40% O_2 at a pressure of 5 Pa and a substrate temperature of 700 °C. During deposition, the substrate holder rotates slowly in order to reduce the dispersion of film thickness over the whole film. After deposition, the films were *in situ* cooled to room temperature and postannealed in air at 700 °C for 30 min using a rapid thermal processor furnace.

X-ray diffraction (XRD) patterns of the $LaMnO_{3+\delta}$/PMN-PT and $CaMnO_3$/PMN-PT structures were recorded using a four-circle Bruker D8 Discover x-ray diffractometer equipped with Cu $K\alpha_1$ radiation. For *in situ* XRD measurements, the electric potentials applied to the $LaMnO_{3+\delta}$/PMN-PT (or the $CaMnO_3$/PMN-PT) structure was changed from 0 to 10 kV/cm in steps of 0.5 or 1 kV/cm while all other parameters were kept constant after the alignment of the x-ray beam. The measurements were made in the 2θ range from 44° to 50° at 295 K during the application of an electric field E $(0 \leq E \leq 10$ kV/cm) to the $LaMnO_{3+\delta}$/PMN-PT (or the $CaMnO_3$/PMN-PT) structure. A schematic of the electric field configuration for *in situ* XRD measurements is shown in the inset (a) of Fig. 1. XRD θ-2θ scan of the $LaMnO_{3+\delta}$/PMN-PT structure indicates that the $LaMnO_{3+\delta}$ film is c-axis preferentially oriented and has no

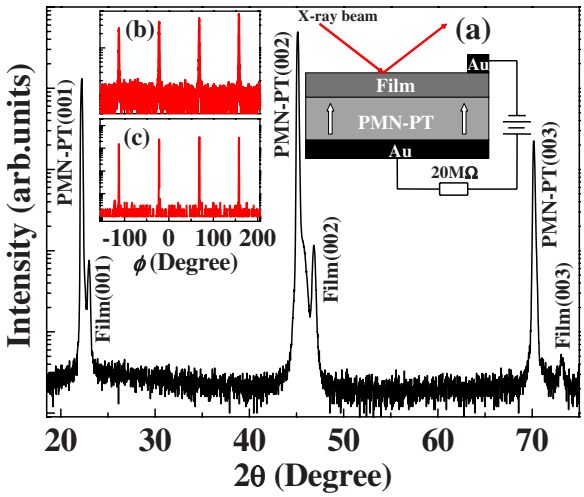

FIG. 1. (Color online) X-ray diffraction pattern of the $LaMnO_{3+\delta}$/PMN-PT structure. Inset (a) shows a schematic of the electric field configuration for *in situ* XRD measurements. The arrow in the inset (a) represents the poling direction. Insets (b) and (c) show the XRD ϕ scans on the $LaMnO_{3+\delta}$(101) and PMN-PT(101) reflections, respectively.

secondary phases (see Fig. 1). We also performed XRD ϕ scans on the $LaMnO_{3+\delta}$(101) and PMN-PT(101) reflections, respectively, and observed a fourfold symmetrical reflection for both the $LaMnO_{3+\delta}$ film and the PMN-PT substrate [insets (b) and (c) of Fig. 1, respectively], indicating the epitaxial growth of the $LaMnO_{3+\delta}$ film on the PMN-PT substrate. Since the dispersion of oxygen content may result in structural inhomogeneity,[8] we thus made XRD measurements on the $LaMnO_{3+\delta}$/PMN-PT structure when the incident x-ray beam is in the longitudinal and transversal configurations with respect to the film square, respectively. We found that the 2θ values of the PMN-PT(002) and $LaMnO_{3+\delta}$(002) reflections for longitudinal configuration are the same as those for transversal configuration, which implies that the dispersion of oxygen content and film thickness over the whole film is small and can be neglected.

The inset (a) of Fig. 2 shows the circuit for electrical resistance measurements. A physical property measurement system (PPMS 9T, Quantum Design) was used to measure the resistance of the $LaMnO_{3+\delta}$ film between the two top-top gold electrodes in the temperature range 10–300 K and in a magnetic field (up to 9 T) applied parallel to the film plane. The resistance of the PMN-PT substrate was estimated to be $\sim 3 \times 10^9$ Ω at room temperature by measuring the leakage current in the PMN-PT substrate using a Keithley 6517A electrometer. Since the resistance ($\sim 1.3 \times 10^4$ Ω at room temperature) of the conducting $LaMnO_{3+\delta}$ (or $CaMnO_3$) film is much smaller than that of the PMN-PT substrate, the $LaMnO_{3+\delta}$ (or the $CaMnO_3$) film, in fact, serves as the top electrode for poling the PMN-PT substrate. This was achieved by applying a dc poling field E (E is much larger than the coercive field E_C of the PMN-PT substrate) to the $LaMnO_{3+\delta}$/PMN-PT (or the $CaMnO_3$/PMN-PT) structure through the film (top electrode) and bottom gold electrodes using a Model PS325 high-voltage power supply (Stanford Research Systems, Inc.). Note that the top electrode was al-

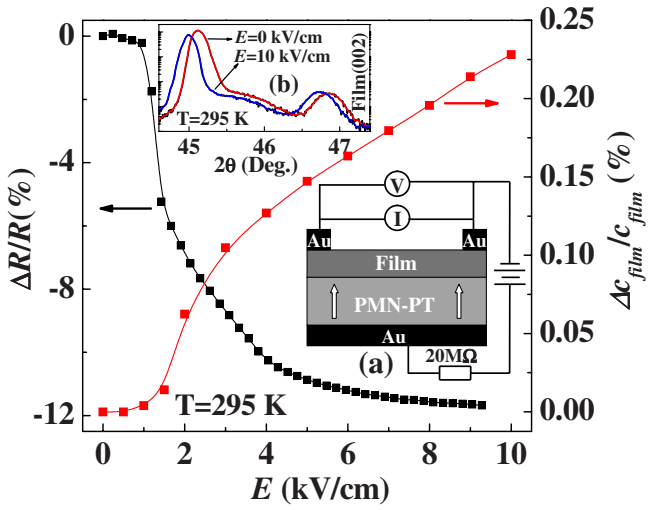

FIG. 2. (Color online) Relative change in the lattice constant c and resistance of the $LaMnO_{3+\delta}$ film as a function of the electric field applied to the $LaMnO_{3+\delta}$/PMN-PT structure through the top and bottom electrodes. Inset (a) shows the circuit for electrical resistance measurements. Inset (b) shows the XRD patterns in the vicinity of (002) reflections for the $LaMnO_{3+\delta}$/PMN-PT structure under zero electric field and an electric field of 10 kV/cm. The initial poling state of the PMN-PT substrate is in P_r^0.

ways held at zero electric potential. The magnetic properties of the $LaMnO_{3+\delta}$ films were measured using a superconducting quantum interference device (SQUID-VSM 7T, Quantum Design) magnetometer with the magnetic field applied parallel to the film plane.

III. RESULTS AND DISCUSSION

A. $LaMnO_{3+\delta}$/PMN-PT structure

1. Effects of ferroelectric poling on the resistance and strain of the film

First, we studied the effects of the strain induced by ferroelectric poling on the transport properties of the $LaMnO_{3+\delta}$ film at a fixed temperature of 295 K. The resistance of the $LaMnO_{3+\delta}$ film between the two top-top gold electrodes was measured as a function of the electric field E applied to the $LaMnO_{3+\delta}$/PMN-PT structure through the top and bottom electrodes. It should be pointed out that initially the PMN-PT substrate was in unpoled state (denoted by P_r^0) and the electric field was increased from 0 to ~9.3 kV/cm in steps of ~0.24 kV/cm. The electric field induced relative change in the resistance, $\Delta R/R$, is plotted as a function of E in Fig. 2. Here, $\Delta R/R$ is defined as $\Delta R/R=[R(E)-R(0)]/R(0)$, where $R(E)$ and $R(0)$ are the resistances of the $LaMnO_{3+\delta}$ film under an electric field E and zero electric field, respectively. The resistance is almost field independent for $E \leq 1$ kV/cm, but decreases drastically with further increase in E. For $E>4$ kV/cm, the resistance decreases gently with increasing E, implying that the poling of the PMN-PT substrate is almost completed below 4 kV/cm. We note that a similar electric field induced decrease in the resistance has been observed in $La_{1-x}Ba_xMnO_3$ $(x=0.125,0.3)$/PMN-PT structure,[13,14] which was found to be due to a change in the strain state of the film induced by ferroelectric poling of the PMN-PT substrate.

We performed *in situ* XRD measurements on a $LaMnO_{3+\delta}$/PMN-PT structure. Selected XRD patterns in the vicinity of the (002) reflection under $E=0$ and 10 kV/cm are shown in the inset (b) of Fig. 2. The results indicate that both the PMN-PT(002) and $LaMnO_{3+\delta}$(002) reflections shift toward lower 2θ values when an electric field E $(E>E_C)$ is applied to the $LaMnO_{3+\delta}$/PMN-PT structure. When the PMN-PT substrate is in P_r^0 state, i.e., $E=0$ kV/cm, the lattice constant c of the $LaMnO_{3+\delta}$ film is calculated to be ~3.875 Å. We recall that the lattice constants of the $LaMnO_{3+\delta}$ bulk materials vary with δ.[3–7] By comparing the onset temperature of ferromagnetic ordering and the charge-ordering transition temperature T_{CO} of the $LaMnO_{3+\delta}$ film (which will be discussed in the following section) with those of $LaMnO_{3+\delta}$ bulk materials,[4,7] it is roughly estimated that the $LaMnO_{3+\delta}$ film has an excess oxygen $\delta \sim 0.09$. For $\delta \sim 0.09$, the lattice constant c of the $LaMnO_{3+\delta}$ single crystal is ~3.903 Å.[4,7] This value is larger than that of the $LaMnO_{3+\delta}$ film, indicating that the film is subjected to an out-of-plane compressive and an in-plane tensile strain, in agreement with the fact that the lattice constants of the $LaMnO_{3+\delta}$ bulk materials are smaller than those $[a \sim b \sim c \sim 4.02$ Å (Ref. 17)] of the PMN-PT substrate.

As can be seen in Fig. 2, the electric field induces a significant increase in the lattice constant c of the $LaMnO_{3+\delta}$ film. c is slightly dependent on E for $E \leq 1$ kV/cm, but increases remarkably with increasing E from 1.5 kV/cm. For $E>4$ kV/cm, c increases almost linearly. We note that, when an electric field of 10 kV/cm is applied to the $LaMnO_{3+\delta}$/PMN-PT structure, the lattice constant c (~3.884 Å) of the film is still smaller than that of the $LaMnO_{3+\delta}$ $(\delta=0.09)$ bulk material, indicating that the film is still under in-plane tensile strain, although the in-plane tensile strain has been considerably reduced. For an unpoled ferroelectric material, the application of an electric field to the material would induce a nonlinear increase in the lattice constants near E_C of the ferroelectric material due to the rotation of the polarization of the ferroelectric domains toward the field direction.[18] The observed nonlinear increase in the lattice constant c of the $LaMnO_{3+\delta}$ film near $E=2$ kV/cm (which is close to E_C of the PMN-PT substrate[14]) is undoubtedly due to the ferroelectric-poling-induced in-plane compressive strain in the PMN-PT substrate. This induced strain was transferred to the film and thus cause a reduction in the in-plane tensile of the film, which reduces the JT distortion of MnO_6 (Ref. 19) and thus a weakening of the electron-lattice coupling, favoring the itinerancy of charge carriers.[20]

We point out that the ferroelectric field effect in the $LaMnO_{3+\delta}$/PMN-PT structure is negligible. If the ferroelectric field effect plays a dominant role in influencing the transport properties of the $LaMnO_{3+\delta}$ film, the resistance electric field (R-E) hysteresis loop should show a squarelike shape with the resistance change exhibiting opposite signs for opposite directions of applied electric field, as previously observed in $La_{1-x}Ba_xMnO_3(x=0.1,0.15)/Pb(Zr_{0.2}Ti_{0.8})TiO_3$ (Ref. 21) and $La_{0.8}Ca_{0.2}MnO_3/Pb(Zr_{0.2}Ti_{0.8})TiO_3$ (Ref. 22)

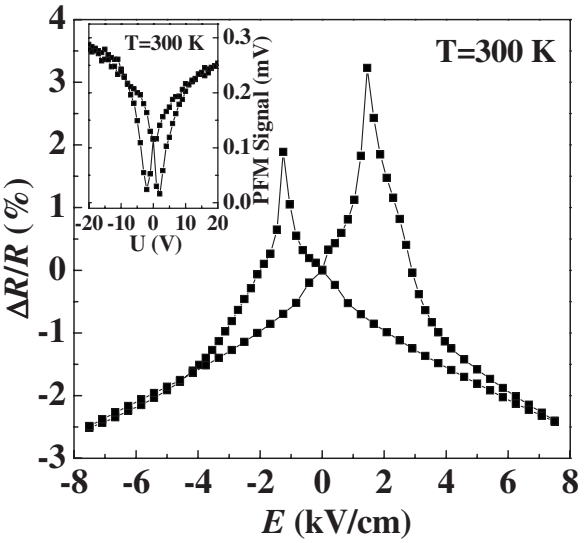

FIG. 3. Relative change in the resistance of the $LaMnO_{3+\delta}$ film between the two top-top gold electrodes at 300 K as a function of bipolar electric field applied to the PMN-PT substrate through the top and bottom electrodes. The PMN-PT substrate was initially in P_r^+ state and the electric field was changed in the sequence of 0 kV/cm→−7.5 kV/cm→+7.5 kV/cm→0 kV/cm. The inset shows the PFM signal (which is in proportional to the induced out-of-plane strain) as a function of bipolar electric potential applied to the PMN-PT substrate.

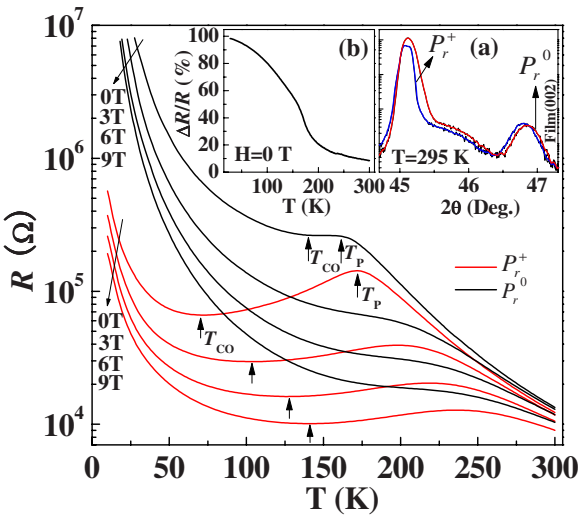

FIG. 4. (Color online) Temperature dependence of the resistance for the $LaMnO_{3+\delta}$ film at $H=0$, 3, 6, and 9 T when the PMN-PT substrate is in P_r^0 and P_r^+ states, respectively. Inset (a) shows the XRD patterns in the vicinity of (002) reflections for the $LaMnO_{3+\delta}$/PMN-PT structure when the PMN-PT substrate is in P_r^0 and P_r^+ states, respectively. Inset (b) shows ferroelectric-poling-induced relative change in the resistance, $\Delta R/R$, of the $LaMnO_{3+\delta}$ film at $H=0$ T. Here, $\Delta R/R$ is defined as $\Delta R/R=[R(P_r^0,H)-R(P_r^+,H)]/R(P_r^0,H)$. Note that the electric field was turned off after the PMN-PT substrate had been poled to P_r^+ state.

ferroelectric field effect transistor structures. However, if the ferroelectric-poling-induced strain plays a dominant role in influencing the transport properties, the *R-E* hysteresis loop should show a butterflylike shape with the resistance change exhibiting the same sign for opposite directions of applied electric field, as previously observed in $La_{0.7}Sr_{0.3}MO_3$(M=Mn,Co)/0.72Pb($Mg_{1/3}Nb_{2/3}$)O_3-0.28$PbTiO_3$ structures.[11,23] We have measured the *R-E* hysteresis loop of the $LaMnO_{3+\delta}$/PMN-PT structure (see Fig. 3). The result shows that the *R-E* hysteresis loop has a butterflylike shape, which is the typical behavior of the resistance change due to the strain induced by the rotation of the polarization direction in the PMN-PT substrate.[11,23] The inset of Fig. 3 shows the electric field induced out-of-plane strain of a PMN-PT single crystal as a function of bipolar electric potential applied to a PMN-PT single crystal, obtained by measurements of the piezoresponse force microscopy (PFM) using a scanning probe microscope operated in the piezoforce mode. Similar to the resistance change shown in Fig. 3, the induced strain shows a butterflylike hysteresis loop, which implies that the butterflylike modulation of the resistance is strain induced. Therefore, we believe that the mechanic distortion of the $LaMnO_{3+\delta}$ film induced by the poling of the substrates plays a dominant role in influencing the transport properties of the $LaMnO_{3+\delta}$ film while the ferroelectric field effect has a minor effect on the electrical properties of the film.

Figure 4 shows the temperature dependence of the resistance for the $LaMnO_{3+\delta}$ film in different magnetic fields H when the PMN-PT substrate is in P_r^0 state and poled state (denoted by P_r^+), respectively. For P_r^0 state and $H=0$ T, the resistance of the film increases with decreasing temperature from 300 K and undergoes an insulator-to-metal like transition at $T_P \sim 161$ K. With further decrease in the temperature, the resistance levels off and increases again at $T \sim 141$ K. The overall behavior is quite similar to that observed in the lightly doped $(La_{0.75}Pr_{0.25})_{7/8}Sr_{1/8}MnO_3$,[24] $La_{1-x}Ca_xMnO_3$ ($x=0.15$ and 0.2),[25] and $La_{1-x}Sr_xMnO_3$ ($0.11 \le x \le 0.13$) (Ref. 26) bulk materials, for which charge/orbital ordering is observed at low temperatures. We note that charge-ordering transition temperatures (T_{CO}) of ~131, 146, and 152 K for $\delta=0.085$, 0.092, and 0.096, respectively, have been observed in $LaMnO_{3+\delta}$ single crystals by Choi *et al.*[7] Ritter *et al.*[3] also observed the CO phase at temperatures below T_C in $LaMnO_{3+\delta}$ ($\delta=0.07$ and 0.1) polycrystalline samples by measurements of ac initial magnetic susceptibility and neutron diffraction. The upturn of the resistance near $T \sim 141$ K in the present $LaMnO_{3+\delta}$ film is probably due to charge ordering. When the magnetic field is increased, the resistance decreases significantly, thus exhibiting colossal magnetoresistance effect. The insulator-to-metal transition temperature also shifts to a higher temperature.

After the measurements of the resistance as a function of temperature in magnetic fields when the PMN-PT substrate was in P_r^0 state, we applied a dc poling field of +10 kV/cm to the $LaMnO_{3+\delta}$/PMN-PT structure through the top and bottom electrodes so that the PMN-PT substrate was poled to P_r^+ state, as schematically indicated by the arrow in the inset (a) of Fig. 2. It should be pointed out that, after the PMN-PT substrate had been poled to P_r^+ state, the poling field applied to the $LaMnO_{3+\delta}$/PMN-PT structure was turned off. Since the PMN-PT substrate has a ferroelectric Curie temperature of ~155 °C (much higher than room temperature), the po-

larization direction will remain toward the poling direction even if the poling field was turned off. As a consequence, there is a remnant strain in the PMN-PT substrate. *In situ* XRD measurements indicate that, associated with the change in the poling state from P_r^0 to P_r^+ (here, $E=0$ kV/cm), both the PMN-PT(002) and $LaMnO_{3+\delta}$(002) reflections shift to lower 2θ values [see the inset (a) of Fig. 4], implying that the lattice constants c of both the PMN-PT substrate and $LaMnO_{3+\delta}$ film have been elongated as a result of ferroelectric poling. The lattice constant c of the film (c_{film}) is found to increase from 3.875 Å for P_r^0 state to 3.880 Å for P_r^+ state, corresponding to $\Delta c_{film}/c_{film} \sim 0.13\%$. Due to the Poisson effect, the increase in $\Delta c_{film}/c_{film}$ would be accompanied by a decrease in the in-plane tensile strain. As a result, the insulator-to-metal like transition temperature T_P increases from 161 to 172 K, and the resistance at $H=0$ T for P_r^+ state becomes smaller than that for P_r^0 state over the whole temperature range (see Fig. 4). The relative change in the resistance, $\Delta R/R$, defined as $\Delta R/R=[R(P_r^0,H)-R(P_r^+,H)]/R(P_r^0,H)$, is shown in the inset (b) of Fig. 4. It is noted that $\Delta R/R$ increases with decreasing temperature, reaching a high value of 98.2% at 30 K. Moreover, T_{CO} (defined as the temperature where the resistance shows an upturn), decreases from 141 to 70 K when the polarization states change from P_r^0 to P_r^+. This, together with the large decrease in the resistance indicates that the CO phase in the $LaMnO_{3+\delta}$ film is substantially suppressed while the FM metallic phase is stabilized as a consequence of the decrease in the JT distortion due to the reduction in the in-plane tensile strain.

Another important feature of the transport properties is that, whether the PMN-PT substrate is in P_r^0 or P_r^+ state, both T_{CO} and T_P increase significantly with increasing magnetic field, and this effect is particularly noticeable when the PMN-PT substrate is in P_r^+ state. This feature is similar to that observed in lightly doped $La_{7/8}Sr_{1/8}MnO_3$ single crystals for which both T_{CO} (near 150 K) and T_P (near 196 K) increase with increasing magnetic fields.[27] The similarity in the effects of magnetic field on both T_{CO} and T_P observed in the $LaMnO_{3+\delta}$ film and the charge-ordered $La_{7/8}Sr_{1/8}MnO_3$ single crystals provides an indirect evidence that the upturn of the resistance near 141 K for P_r^0 state and 71 K for P_r^+ state is associated with a charge-/orbital-ordering phase transition. We note that there are no structural anomalies near $T=141$ and 71 K for the PMN-PT substrate, as revealed by low-temperature XRD measurements.[17]

Figure 5 shows the temperature dependence of the zero-field-cooled (ZFC) and field-cooled (FC) magnetization for the $LaMnO_{3+\delta}$/PMN-PT structure when the PMN-PT substrate is in P_r^0 state. The onset of the ferromagnetic ordering occurs at $T \sim 165$ K, which is close to the insulator-to-metal like transition at $T \sim 161$ K. With decreasing temperature from 165 K, a pronounced irreversibility is observed at $T_{CG} \sim 127$ K between ZFC and FC curves (at $H=50$ G), which is the typical behavior of a magnetic cluster-glass phase, as previously reported for $LaMnO_{3+\delta}$.[28,29] As the field increases the irreversible behavior is reduced and is no longer present at $H=500$ G. The cluster-glass behaviors imply that phase-separation exists (i.e., FM metallic clusters are embedded in an AFM insulating matrix) in the $LaMnO_{3+\delta}$ film at low temperatures. Since the excess oxygen ions cannot be accommodated in the interstitial sites of the perovskite structure, the oxidation process is, in fact, accomplished through the formation of equal amounts of La and Mn vacancies.[30] To maintain the charge neutrality, some of Mn^{3+} ions would be oxidized to Mn^{4+} ions. Trapping of Mn^{4+} ions near the cation vacancies introduces local FM metallic clusters within which electron transfer from Mn^{3+} to Mn^{4+} ions introduces FM double-exchange interaction that is stronger than the AFM Mn^{3+}-O-Mn^{3+} superexchange interaction in the host lattice.[31] Because the concentration of Mn vacancies and, hence, of clusters is not high, these FM metallic clusters are separated from one another, giving rise to FM insulating behavior of the resistance at $H=0$ T when the PMN-PT substrate is in P_r^0 state. Nevertheless, associated with the decrease in the electron-lattice coupling due to the reduced in-plane tensile strain in the film, the enhanced hopping of the charge carriers makes it possible for the FM metallic clusters grow in size and merge into larger clusters, causing a large decrease in the resistance at low temperatures and a shift of T_{CO} toward lower temperatures.

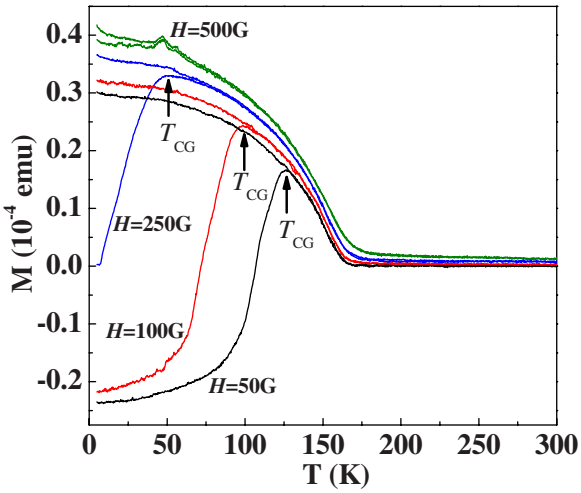

FIG. 5. (Color online) Temperature dependence of the zero-field-cooled (ZFC) and field-cooled (FC) magnetization for the $LaMnO_{3+\delta}$ film when the PMN-PT substrate is in P_r^0 state.

The ferroelectric-poling-induced strain also has a remarkable influence on the magnetotransport properties of the $LaMnO_{3+\delta}$ film. In Fig. 6, we present the temperature dependence of the MR at $H=3$, 6, and 9 T for the $LaMnO_{3+\delta}$ film when the PMN-PT substrate is in P_r^0 and P_r^+ states, respectively. Here, MR is defined as $MR=[R(0)-R(H)]/R(0)$, where $R(0)$ and $R(H)$ are the resistance of the film in zero magnetic field and a magnetic field H, respectively. It is interesting that, for any H value, the MR versus T curves for P_r^0 and P_r^+ states have a crossover, indicating that a reduction in the in-plane tensile strain leads to opposite effects on MR, namely, MR is reduced in the low-temperature FM state while MR is enhanced in the high-temperature paramagnetic (PM) state.

To better characterize the effects of the induced strain on MR, we measured MR of the film at various fixed temperatures covering the range from the FM state to PM state. In the inset of Fig. 6, we show the MR versus H curves at 40

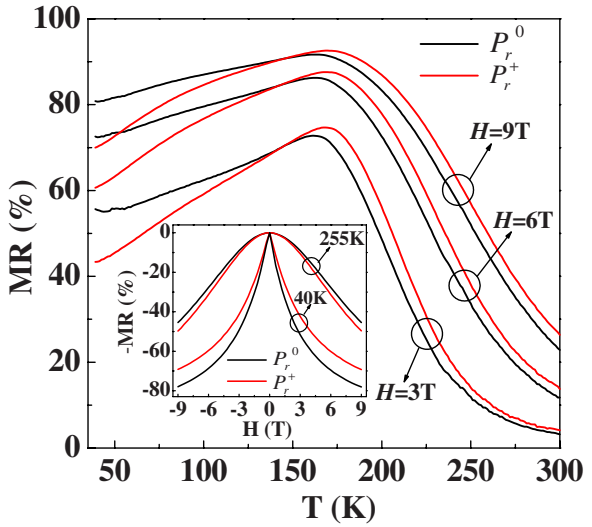

FIG. 6. (Color online) Temperature dependence of MR for the $LaMnO_{3+\delta}$ film at $H=3$, 6, and 9 T when the PMN-PT substrate is in P_r^0 and P_r^+ states, respectively. Inset shows MR versus H curves at $T=40$ and 255 K for the $LaMnO_{3+\delta}$ film when the PMN-PT substrate is in P_r^0 and P_r^+ states, respectively.

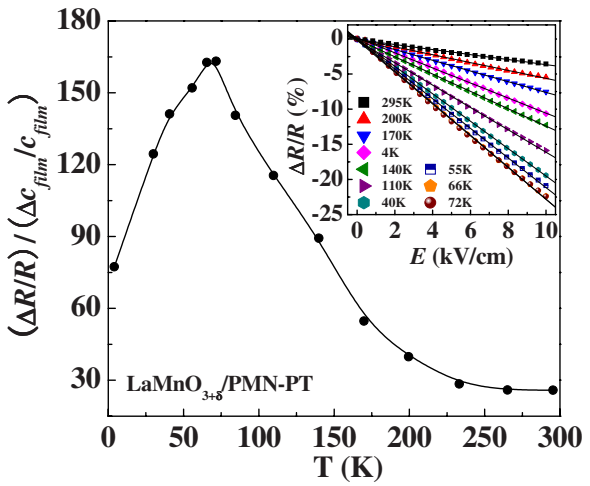

FIG. 7. (Color online) Temperature dependence of the resistance-strain coefficient of the $LaMnO_{3+\delta}$ film. The inset shows the relative change in the resistance, $\Delta R/R$, of the $LaMnO_{3+\delta}$ film between the two top-top gold electrodes as a function of the electric field applied to the $LaMnO_{3+\delta}$/PMN-PT structure through the top and bottom electrodes.

and 255 K when the PMN-PT substrate is in P_r^0 and P_r^+ states, respectively. The results clearly indicate that, in comparison with the MR when the PMN-PT substrate is in P_r^0 state, the MR value when the PMN-PT substrate is in P_r^+ state is reduced in the FM state (e.g., 40 K) but enhanced in the PM state, consistent with the behavior of the MR versus T curves shown in Fig. 6. Note that the induced strain has opposite effects on MR in FM and PM states was previously observed for the $La_{0.7}Ba_{0.3}MnO_3$/PMN-PT structure.[15] The similarity in the behavior of MR between $LaMnO_{3+\delta}$ and $La_{0.7}Ba_{0.3}MnO_3$ films implies that the underlying mechanism is probably the same. Namely, the effects of the induced strain on MR can be explained in terms of phase separation. In the high-temperature PM insulating state, it is reasonable that a small fraction of FM metallic clusters arising from the local Mn^{3+}-O-Mn^{4+} double exchange are embedded in the PM insulating matrix. Associated with the reduction in the JT distortion induced by the ferroelectric poling, the volume fraction of the FM metallic phase would increase at the expense of the PM insulating phase. As a consequence, MR for P_r^+ state is larger than that for P_r^0 state in the high-temperature PM state.[15]

In the low-temperature FM state, e.g., $T=30$ K, the CO insulating phase coexists with the FM metallic phase with the former dominating over the latter. It is noted that, in the CO state, MR results largely from the magnetic field induced conversion of CO insulating phase to FM metallic phase.[32–34] The large decrease in the resistance (e.g., $\Delta R/R \approx 98.2\%$ at 30 K) induced by ferroelectric poling [inset (b) of Fig. 4] indicates that a considerable fraction of the CO insulating phase have been converted to FM metallic phase due to the decrease in the in-plane tensile strain. That is, the volume fraction of the CO insulating phase in P_r^+ state is smaller than that in P_r^0 state. Therefore, the effective volume fraction of the CO insulating phase that is converted to FM metallic phase in P_r^+ state would be smaller than that in P_r^0 state. So, the MR in P_r^+ state is smaller than that in P_r^0 state. We mention here that similar phenomena have been observed in charge-ordered $Pr_{0.5}Ca_{0.5}Mn_{1-x}Cr_xO_3$ $(0 \le x \le 0.07)$,[32] $La_{0.625-x}Pr_xCa_{0.325}MnO_3$,[33] and $Pr_{0.5}Ca_{0.2}Sr_{0.3}MnO_{3-\delta}$ (Ref. 34) systems in which the low-temperature MR decreases with increasing volume fraction of FM metallic phase induced by Cr (or La) doping or oxygen deficiencies.

2. Effects of the converse piezoelectric effect on the resistance and strain of the film

After the PMN-PT substrate had been poled to P_r^+ state, we studied the effects of the strain induced by the converse piezoelectric effect on the strain state and transport properties of the $LaMnO_{3+\delta}$ film. The inset of Fig. 7 shows the relative change in the resistance, $\Delta R/R$, of the film between the two top-top gold electrodes as a function of the electric field applied to the $LaMnO_{3+\delta}$/PMN-PT structure through the top and bottom electrodes. One sees that $\Delta R/R$ decreases linearly with increasing electric field at any fixed temperature. Since there are considerable amount of La and Mn vacancies in the film, it is naturally expected that some of these vacancies and/or some lattice-mismatch-induced dislocations would appear at the interface between the film and the substrate, whose state may be affected by the induced strain, thereby influencing the transport properties. Nevertheless, we found that the linear dependence of the resistance on E can be quite well reproduced. We thus believe that the effects of vacancies and/or dislocations on the resistance can be neglected when the strain state of the film is modified by the applied electric field. It is well known that, when an electric field is applied to a poled ferroelectric material, a strain along the direction of the electric field would be induced due to the converse piezoelectric effect.[18] The induced strain ε is proportional to the electric field E, i.e., $\varepsilon = d_{33}E$, where d_{33} is the longitudinal piezoelectric coefficient of the poled

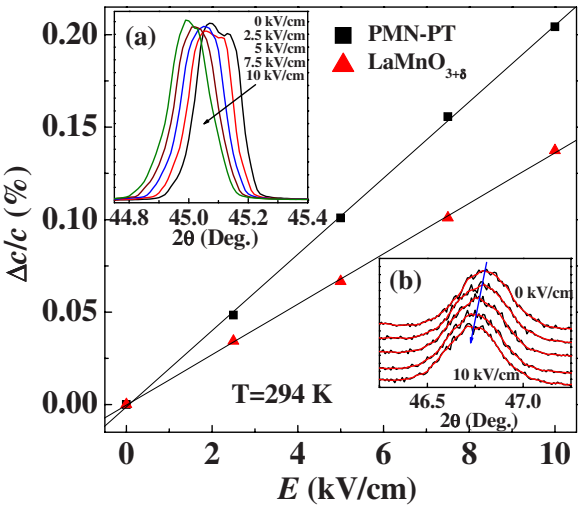

FIG. 8. (Color online) Relative change in the lattice constants c of the PMN-PT substrate and $LaMnO_{3+\delta}$ film as a function of the electric field applied to the $LaMnO_{3+\delta}$/PMN-PT structure. Note that the PMN-PT substrate has already been poled to P_r^+ state before the *in situ* XRD measurements. Insets (a) and (b) show the XRD patterns in the vicinity of (002) reflections for the PMN-PT substrate and $LaMnO_{3+\delta}$ film under different electric fields, respectively.

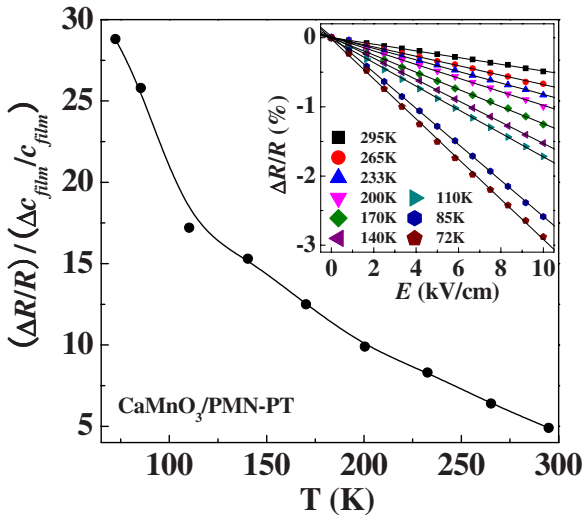

FIG. 9. (Color online) Temperature dependence of the resistance-strain coefficient of the $CaMnO_3$ film. The inset shows the relative change in the resistance, $\Delta R/R$, of the $CaMnO_3$ film between the two top-top gold electrodes as a function of the electric field applied to the $CaMnO_3$/PMN-PT structure through the top and bottom electrodes.

material.[18] *In situ* XRD measurements on a $LaMnO_{3+\delta}$/PMN-PT structure indicate that both the PMN-PT(002) and $LaMnO_{3+\delta}$(002) reflections systematically shift to lower 2θ values [see the insets (a) and (b) of Fig. 8, respectively] with increasing electric field, indicating that the lattice constants c of both the PMN-PT substrate and the $LaMnO_{3+\delta}$ film have been elongated. As can be seen in Fig. 8, the relative change in the lattice constant c of the PMN-PT substrate, $\Delta c_{\text{PMN-PT}}/c_{\text{PMN-PT}}$, increases linearly with increasing E, indicating the piezoelectric nature of the induced strain in the substrate.[14] The induced strain was transferred to the film, giving rise to a linear dependence of $\Delta c_{film}/c_{film}$ on E. The relationship between $\Delta R/R$ and $\Delta c_{film}/c_{film}$ can be written as $\Delta R/R = m\Delta c_{film}/c_{film}$, where m is a constant. The resistance-strain coefficient $(\Delta R/R)/(\Delta c_{film}/c_{film})$ of the $LaMnO_{3+\delta}$ film is plotted as a function of temperature in Fig. 7. $(\Delta R/R)/(\Delta c_{film}/c_{film})$ increases with decreasing temperature and reaches a maximal value ($\sim$163) near T_{CO} ($\sim$70 K) and then decreases remarkably with further decreases in the temperature. We note that $(\Delta R/R)/(\Delta c_{film}/c_{film})$ of the $LaMnO_{3+\delta}$ film near T_{CO} is considerably larger than that $[(\Delta R/R)/(\Delta c_{film}/c_{film}) \sim 26-76]$ of $La_{0.7}Ca_{0.15}Sr_{0.15}MnO_3$ thin films grown on PMN-PT substrates.[13] For perovskite manganites exhibiting insulator-to-metal transition, e.g., $La_{0.7}A_{0.3}MnO_3$ (A=Ca, Sr), it is generally accepted that there is strong JT electron-lattice coupling in the PM insulating state and the reduction in the JT electron-lattice coupling is mainly responsible for the large decrease in the resistance just below the insulator-to-metal transition temperature.[1,35–37] The observed large resistance-strain coefficient demonstrates that there exists strong JT electron-lattice coupling in the $LaMnO_{3+\delta}$ film.

B. $CaMnO_3$/PMN-PT structure

To obtain more insight into the effects of the JT electron-lattice coupling on the transport properties of $LaMnO_{3+\delta}$ film, we studied the effects of the strain induced by the converse piezoelectric effect on the transport properties of $CaMnO_3$ thin films grown on PMN-PT substrates and compared the results with that of $LaMnO_{3+\delta}$ films. Similar to that observed in the $LaMnO_{3+\delta}$ film, the resistance of the $CaMnO_3$ film at a fixed temperature also decreases linearly with increasing E, as can be seen in the inset of Fig. 9. Although the relative change in the resistance, $\Delta R/R$, is relatively small, the results clearly indicate that a reduction in the in-plane tensile strain leads to a decrease in the resistance of the $CaMnO_3$ film. Based on *in situ* XRD measurements, we found that, when an electric field of 10 kV/cm is applied to the $CaMnO_3$/PMN-PT structure, the relative change in the lattice constant c of the $CaMnO_3$ film, $\Delta c_{film}/c_{film}$, is $\sim$0.1%. The resistance-strain coefficients, $(\Delta R/R)/(\Delta c_{film}/c_{film})$, of the $CaMnO_3$ film at various temperatures are calculated and shown in Fig. 9. It was found that, at the same temperature, $(\Delta R/R)/(\Delta c_{film}/c_{film})$ of the $LaMnO_{3+\delta}$ film is much larger than that of the $CaMnO_3$ film. Since the $CaMnO_3$ film does not show JT distortion, the effects of JT electron-lattice coupling on the transport properties in $CaMnO_3$ film can be neglected. The linearly decrease in the resistance of the $CaMnO_3$ film probably arises from an increase in the electronic bandwidth due to the reduction in the in-plane tensile strain, which leads to a change in the Mn-O bond length and/or the Mn-O-Mn bond angle. It is worth mentioning that the experimental works by Chen *et al.*[38,39] showed that, in lightly doped $La_{0.9}Sr_{0.1}MnO_3$ thin films, the electron-lattice coupling stemming from the JT distortion is mainly responsible for the effects of substrate-induced strain on the transport and magnetic properties of the film and that the contribution from the electronic bandwidth is much smaller than that from the electron-lattice coupling. We thus believe that the strain-induced modification in the electronic bandwidth alone is not sufficient to account for the

large $(\Delta R/R)/(\Delta c_{film}/c_{film})$ observed in the $LaMnO_{3+\delta}$ film. The effects of the induced strain on the transport properties of the $LaMnO_{3+\delta}$ film is mainly due to the strain-induced weakening of the electron-lattice coupling arising from the reduction in the in-plane tensile strain. This result is in agreement with the theoretical calculation by Ahn and Millis,[40,41] who showed that the strong coupling between electron and lattice is crucial for the understanding of the effects of substrate-induced strain in $LaMnO_3$ thin films.

IV. CONCLUSIONS

In summary, using ferroelectric PMN-PT single crystals as substrates, we have studied the effects of the substrate-induced strain on the strain state and transport properties of $LaMnO_{3+\delta}$ thin films by *in situ* dynamically modifying the lattice strain of the films via ferroelectric poling or the converse piezoelectric effect. Ferroelectric poling (or the converse piezoelectric) induces a significant decrease in the in-plane tensile strain of the film, which reduces the JT electron-lattice coupling, thereby enhancing the volume fraction of the FM metallic phase. As a result, the resistance was reduced; the insulator-to-metal transition temperature T_P was enhanced. Particularly, it was observed that the decrease in the in-plane tensile strain leads to opposite effects on MR above and below T_P, which is found to be closely related to the strain-induced changes in the volume fraction of coexistence phases. Moreover, we have observed that the resistance-strain coefficient $(\Delta R/R)/(\Delta c_{film}/c_{film})$ of $LaMnO_{3+\delta}$ films is much larger than that of $CaMnO_3$ films (for which there is no JT distortion), identifying that the JT distortion plays a very important role in determining the transport properties of $LaMnO_{3+\delta}$ films. The results also show that the strong coupling between electron and lattice is crucial for the understanding of the effects of substrate-induced strain in manganite thin films.

ACKNOWLEDGMENTS

This work was supported by the Max Planck Institute for Solid State Research, the Hong Kong Research Grants Council under Grant No. CERG PolyU 5122/07E, and the Center for Smart Materials of the Hong Kong Polytechnic University. One of us (R.K.Z.) is highly indebted to the Alexander von Humboldt Foundation.

[1] M. B. Salamon and M. Jamie, Rev. Mod. Phys. **73**, 583 (2001).
[2] Y. Murakami, J. P. Hill, D. Gibbs, M. Blume, I. Koyama, M. Tanaka, H. Kawata, T. Arima, Y. Tokura, K. Hirota, and Y. Endoh, Phys. Rev. Lett. **81**, 582 (1998).
[3] C. Ritter, M. R. Ibarra, J. M. De Teresa, P. A. Algarabel, C. Marquina, J. Blasco, J. Garíca, S. Oseroff, and S.-W. Cheong, Phys. Rev. B **56**, 8902 (1997).
[4] F. Prado, R. D. SaHnchez, A. Caneiro, M. T. Causa, and M. Tovar, J. Solid State Chem. **146**, 418 (1999).
[5] J. Töpfer and J. B. Goodenough, J. Solid State Chem. **130**, 117 (1997).
[6] D. Louca, E. L. Brosha, and T. Egami, Phys. Rev. B **61**, 1351 (2000).
[7] K.-Y. Choi, Y. G. Pashkevich, V. P. Gnezdilov, G. Güntherodt, A. V. Yeremenko, D. A. Nabok, V. I. Kamenev, S. N. Barilo, S. V. Shiryaev, A. G. Soldatov, and P. Lemmens, Phys. Rev. B **74**, 064406 (2006).
[8] I. O. Troyanchuk, V. A. Khomchenko, M. Tovar, H. Szymczak, and K. Bärner, Phys. Rev. B **69**, 054432 (2004).
[9] X. O. Bilani-Zeneli, A. D. Rata, A. Herklotz, O. Mieth, L. M. Eng, L. Schultz, M. D. Biegalski, H. M. Christen, and K. Dörr, J. Appl. Phys. **104**, 054108 (2008).
[10] R. B. Gangineni, L. Schultz, C. Thiele, I. Mönch, and K. Dörr, Appl. Phys. Lett. **91**, 122512 (2007).
[11] C. Thiele, K. Dörr, S. Fähler, L. Schultz, D. C. Meyer, A. A. Levin, and P. Paufler, Appl. Phys. Lett. **87**, 262502 (2005).
[12] C. Thiele, K. Dörr, O. Bilani, J. Rödel, and L. Schultz, Phys. Rev. B **75**, 054408 (2007).
[13] R. K. Zheng, Y. Jiang, Y. Wang, H. L. W. Chan, C. L. Choy, and H. S. Luo, Appl. Phys. Lett. **93**, 102904 (2008).
[14] R. K. Zheng, Y. Wang, H. L. W. Chan, C. L. Choy, and H. S. Luo, Appl. Phys. Lett. **92**, 082908 (2008).
[15] R. K. Zheng, Y. Jiang, Y. Wang, H. L. W. Chan, C. L. Choy, and H. S. Luo, Phys. Rev. B **79**, 174420 (2009).
[16] Z. W. Yin, H. S. Luo, P. C. Wang, and G. S. Xu, Ferroelectrics **229**, 207 (1999).
[17] B. Noheda, D. E. Cox, G. Shirane, J. Gao, and Z.-G. Ye, Phys. Rev. B **66**, 054104 (2002).
[18] B. Jaffe, W. R. Cook, Jr., and H. Jaffe, *Piezoelectric Ceramics* (Academic Press, New York, 1971).
[19] N. M. Souza-Neto, A. Y. Ramos, H. C. N. Tolentino, E. Favre-Nicolin, and L. Ranno, Phys. Rev. B **70**, 174451 (2004).
[20] A. J. Millis, T. Darling, and A. Migliori, J. Appl. Phys. **83**, 1588 (1998).
[21] T. Kanki, Y.-G. Park, H. Tanaka, and T. Kawai, Appl. Phys. Lett. **83**, 4860 (2003).
[22] T. Zhao, S. B. Ogale, S. R. Shinde, R. Ramesh, R. Droopad, J. Yu, K. Eisenbeiser, and J. Misewich, Appl. Phys. Lett. **84**, 750 (2004).
[23] A. D. Rata, A. Herklotz, K. Nenkov, L. Schultz, and K. Dörr, Phys. Rev. Lett. **100**, 076401 (2008).
[24] J. Geck, P. Wochner, S. Kiele, R. Klingeler, A. Revcolevschi, M. v. Zimmermann, B. Büchner, and P. Reutler, New J. Phys. **6**, 152 (2004).
[25] G.-L. Liu, J.-S. Zhou, and J. B. Goodenough, Phys. Rev. B **70**, 224421 (2004).
[26] B. Dabrowski, X. Xiong, Z. Bukowski, R. Dybzinski, P. W. Klamut, J. E. Siewenie, O. Chmaissem, J. Shaffer, C. W. Kimball, J. D. Jorgensen, and S. Short, Phys. Rev. B **60**, 7006 (1999).
[27] S. Uhlenbruck, R. Teipen, R. Klingeler, B. Büchner, O. Friedt, M. Hücker, H. Kierspel, T. Niemöller, L. Pinsard, A. Revcolevschi, and R. Gross, Phys. Rev. Lett. **82**, 185 (1999).
[28] S. N. Barilo, V. I. Gatal'skaya, S. V. Shiryaev, G. L. Bychkov, L. A. Kurochkin, S. N. Ustinovich, R. Szymczak, M. Baran, and B.

Krzymańska, Phys. Solid State **45**, 146 (2003).
[29] L. Ghivelder, I. A. Castillo, M. A. Gusmão, J. A. Alonso, and L. F. Cohen, Phys. Rev. B **60**, 12184 (1999).
[30] J. A. M. van Roosmalen and E. H. P. Cordfunke, J. Solid State Chem. **110**, 109 (1994).
[31] J. Töpfer and J. B. Goodenough, Chem. Mater. **9**, 1467 (1997).
[32] S. X. Cao, W. J. Li, J. C. Zhang, B. J. Kang, T. Gao, and C. Jing, J. Appl. Phys. **102**, 053909 (2007).
[33] M. Uehara, S. Mori, C. H. Chen, and S.-W. Cheong, Nature (London) **399**, 560 (1999).
[34] D. Niebieskikwiat, A. Caneiro, and R. D. Sánchez, J. Appl. Phys. **93**, 8080 (2003).
[35] A. J. Millis, P. B. Littlewood, and B. Shraiman, Phys. Rev. Lett. **74**, 5144 (1995).
[36] A. J. Millis, Nature (London) **392**, 147 (1998).
[37] C. H. Booth, F. Bridges, G. H. Kwei, J. M. Lawrence, A. L. Cornelius, and J. J. Neumeier, Phys. Rev. Lett. **80**, 853 (1998).
[38] X. J. Chen, S. Soltan, H. Zhang, and H.-U. Habermeier, Phys. Rev. B **65**, 174402 (2002).
[39] X. J. Chen, H.-U. Habermeier, H. Zhang, G. Gu, M. Varela, J. Santamaria, and C. C. Almasan, Phys. Rev. B **72**, 104403 (2005).
[40] K. H. Ahn and A. J. Millis, Physica B **312-313**, 766 (2002).
[41] K. H. Ahn and A. J. Millis, Phys. Rev. B **64**, 115103 (2001).